Interferometer Topology Decision: Summary and View Graphs, Sept. 30, 1993

Circulated by L. Sievers, 10/15/93

Distribution:

A. Abramovici
W. Althouse
J. Camp
P. Fritschel
J. Giaime
Y. Hefetz
S. Kawamura
A. Kuhnert
M. Regehr
R. Savage
V. Schmidt
D. Shoemaker
L. Sievers
R. Spero
K. Thorne
R. Vogt
R. Weiss
S. Whitcomb
M. Zucker

File:

Caltech
MIT

LIGO-G930062-00-D

Interferometer Topology Decision:
Summary & Viewgraphs

Sept. 30, 1993

to: LIGO science team
from: R. Weiss October 11, 1993
Modified by Lisa Sievers October 13,1993
concerning: Summary of the interferometer topology decision

The LIGO science team met at Caltech on September 30, 1993 to consider the recommendation made by Joe Giaime, Fred Raab, Martin Regehr, David Shoemaker and Lisa Sievers on the interferometer design to pursue for detailed study and research as the initial LIGO interferometer. The recommendation of the group was accepted by the LIGO project.

The concept of the proposed interferometer

1) The design is a power recycled Michelson/Fabry-Perot interferometer using external phase modulation of the carrier and a frequency shifted sub-carrier for signal extraction. The carrier and sub-carrier with their associated phase modulated sidebands are transmitted through an input mode filter cavity before injection into the interferometer.

2) The carrier is resonant in the recycled Michelson interferometer as well as the arm cavities. The sub-carrier and the phase modulation sidebands of both the carrier and the sub-carrier are resonant only in the recycled Michelson interferometer.

3) The discriminant for measurement and control of differential motion (GW signal) of the arm cavities is detected at the antisymmetric port of the interferometer by a deliberate asymmetry in the Michelson paths. The control signal is derived from the carrier and its sidebands.

4) Two schemes for reading out the discriminants of the common mode motion of the arm cavities and differential and common mode motion of the Michelson interferometer paths will be developed to the point of operational systems:

a) Subcarrier scheme: The common mode arm cavity signal is generated from light reflected by the recycling cavity using the carrier and its sidebands. The common mode Michelson signal is also generated from light reflected from the recycling cavity, but using the sub-carrier and its sidebands. The differential Michelson signal is detected at the interferometer antisymmetric port using the sub-carrier and its sidebands.

b) Asymmetry scheme: All signals are derived from the carrier and its sidebands. The common mode arm cavity signal and differential mode Michelson signal are detected at a pick-off inside the recycling cavity; the common mode arm cavity signal is derived from an in-phase demodulation while the differential mode Michelson signal is detected by quadrature phase demodulation of the light. The common mode Michelson signal is detected in the light reflected by the recycling cavity.

5) A laser frequency trim control signal is derived from the average lengths of the 4km arm cavities in either readout scheme.

6) An output spatial mode filter at the antisymmetric port is likely to be required.

Issues requiring further study and design

1) Make preliminary decision on the control strategy for the interferometer.

2) An integrated experiment plan to test the interferometer concept in the suspended prototypes.

3) The method of generating the sub-carrier.

4) The concept and design of an output filter.

5) The sensitivity of the interferometer to the cross terms from amplitude fluctuations of the laser light with the phase and amplitude modulation sidebands of the electro-optic modulator.

6) The sensitivity of the design to mirror and coating errors

7) The noise budget of the design: propagation of noise in the control loops into the gravitational wave signal with specific attention to the influence of optical system imperfections.

8) A model for the interferometer alignment system including the influence of wavefront errors from the mirrors and coatings.

9) The development of a combined optical and control model for the length and angular control for small pertubations around the interferometer operating point.

10) A model and the development of a procedure for the lock acquisition of the interferometer.

MEETING AGENDA FOR DECISION ON LIGO INTERFEROMETER
MODULATION AND TOPOLOGY SCHEME
(September 30, 1993)

I. Intro/Overview (DHS ~ 20 min)
   a. Purpose of Mod Top effort
   b. Description of GW sensing, and aux sensing for lock and operation
   c. Overview of what will be discussed

II. Discussion of Assymetry Scheme (MR ~ 20 min)
   a. layout
   b. method for GW sensing
   c. method for aux sensing
   d. locking techniques

III. Discussion of MZ/Subcarrier Scheme (JG ~ 20 min)
   a. layout
   b. method for GW sensing
   c. method for aux sensing
   d. locking techniques

IV. Experiments and Modeling (MR ~ 20 min)
   a. shot noise
   b. LF and HF response (JG for subcarrier scheme)
   c. calculation for assymetry noise coupling (FJR)

V. Open Issues (DHS ~ 20 min)
   a. Subcarrier scheme
      i. sensitivity of FSS signals to arm cavitites
      ii. spatial mode concerns and numerical modeling
      iii. fitting FSS frequencies through MC
   b. Assymetry scheme
      - servo loop design for assym (LS)
   c) Method for generating FSS

VI. Recommendation of hybrid schemes for LIGO (DHS/FJR ~ 30 min)

VII. Future R&D, work to be done, time and manpower estimates
   a. FMI work (MR/JG ~ 5 min)
   b. Modeling and servo analysis (LS/YH ~ 5 min)
   c. Tests on hanging interferometers
      i. 5 M shot noise tests (PF ~ 5 min)
      ii. 40 M system tests (FJR ~ 5min)

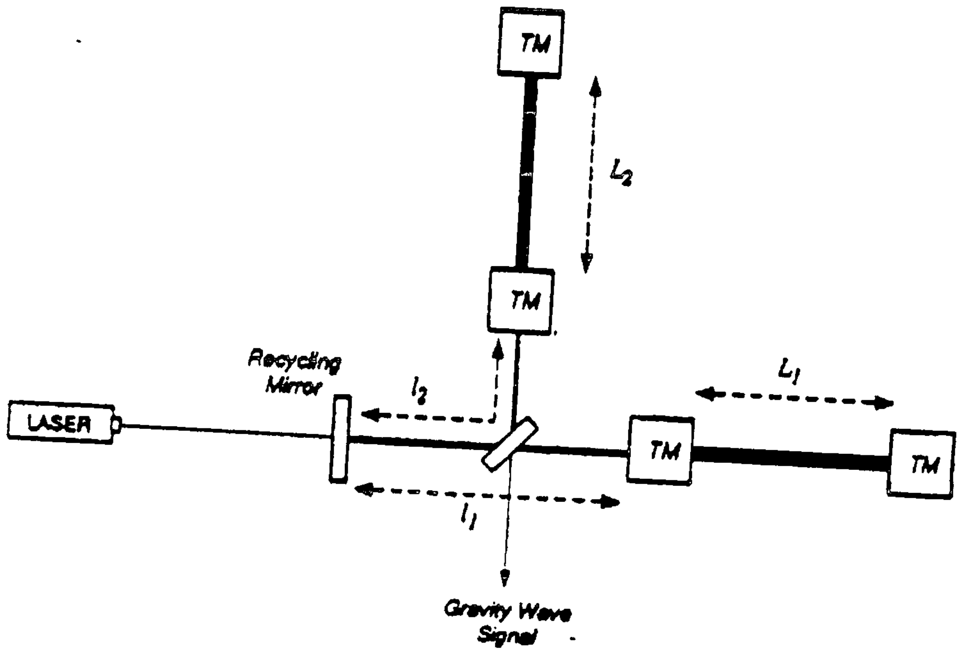

- Point of departure:
  - Michelson interferometer, Fabry-Perot cavities in arms
  - 'Recycling' of laser light (increase in effective power)
- Significant lengths:
  - Cavity 1, Cavity 2
  - recycling cavity resonance
  - Michelson dark fringe
- Better: 4 degrees of freedom
  - differential motion of cavities (GW signal)
  - common mode motion of cavities, differential and common mode of Michelson

I. Intro/Overview

Interferometer Modulation and Topology Review

- Need to define an initial LIGO interferometer layout, control system
- early Fixed Mass Interferometer (FMI) tests
  - recombined Michelson (MI) with Fabry-Perot (FP) arms
  - recycling, consequences of coupled cavities
- Several candidate schemes proposed
  - various means of GW readout, sensing of other lengths
- Leads to present effort
  - (FMI) experiments of complete trial schemes
  - modeling (analytic, numeric)
  - many contributors at different times
- Today:
  - Presentation of status, experiment and modeling
  - discussion of problems, missing information, consequences
  - recommendation for scheme to pursue

II. Asymmetry Scheme

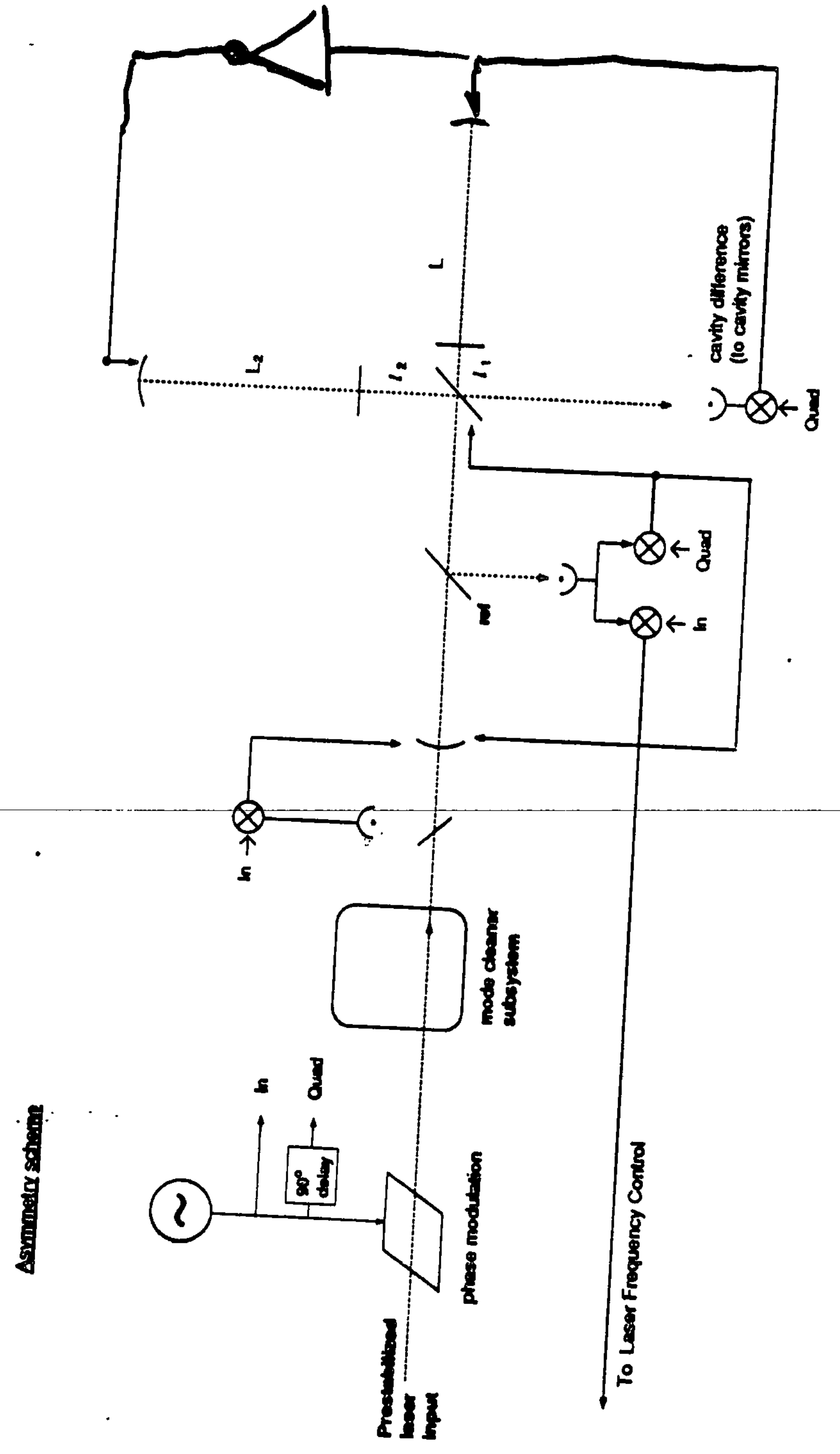

Brief Review of Phase and Amplitude Modulation

Light incident on interferometer is phase modulated at Radio Frequency (RF):

electric field — phase modulation

$$\mathbf{E}(t) = Re\{Ee^{i2\pi\nu t}e^{i\Gamma\sin\omega t}\}$$

~ $10^7 s^{-1}$

$$\simeq Re\{(E_0 + E_+e^{+i\omega t} + E_-e^{-i\omega t})e^{i2\pi\nu t}\}$$

slowly varying envelope

$$E_0 = J_0(\Gamma)$$
$$E_+ = J_1(\Gamma)$$
$$E_- = -J_1(\Gamma)$$

Carrier light plus two RF sidebands.

Draw components of 'envelope' phasor in complex plane:

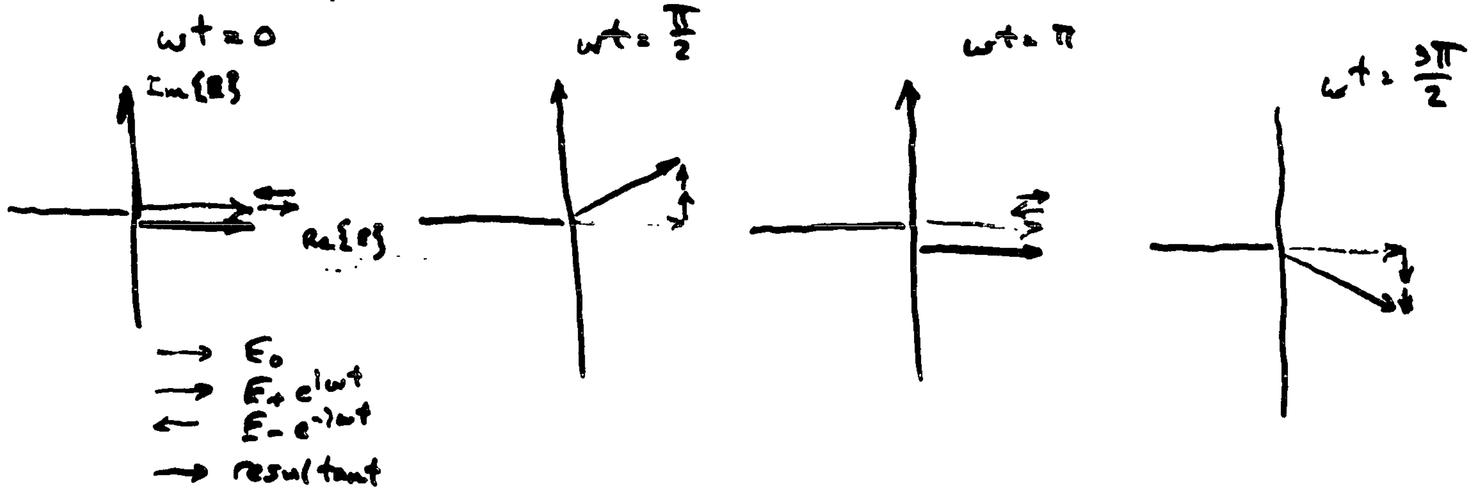

To first order, only phase of envelope phasor changes.

Asymmetry Scheme

Now suppose E_0 phase changes relative to phase of E_+ and E_-. Then

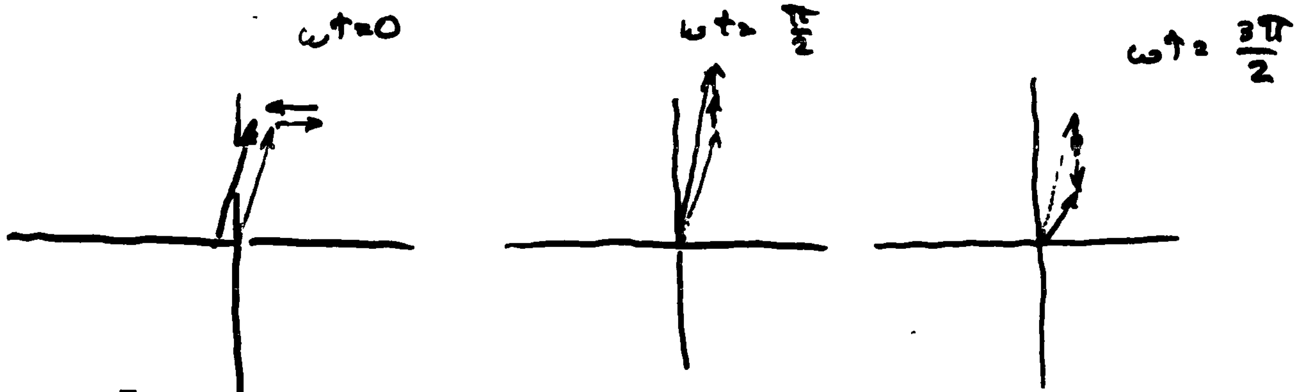

- Envelope amplitude is modulated. This can be detected with a photodiode.

If one sideband is bigger than the other,

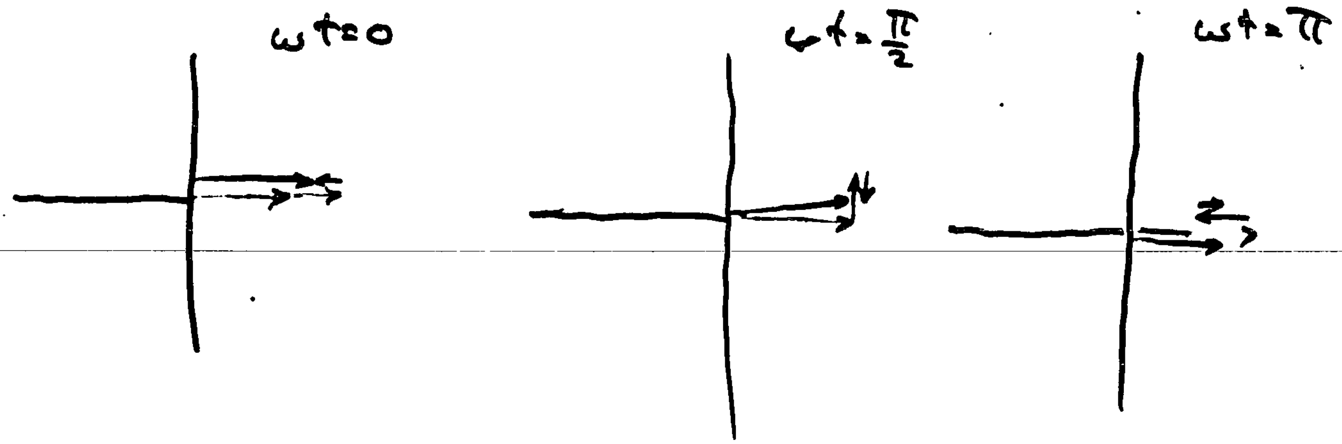

- Envelope amplitude modulated.

Summary:

➜ AM produced when relative phase of carrier and sidebands changes, or when the relative amplitude of the RF sidebands changes.

Asymmetry Scheme

Gravitational Wave Sensing

(Schnupp, '86 or '87)

Symmetric Michelson interferometer:

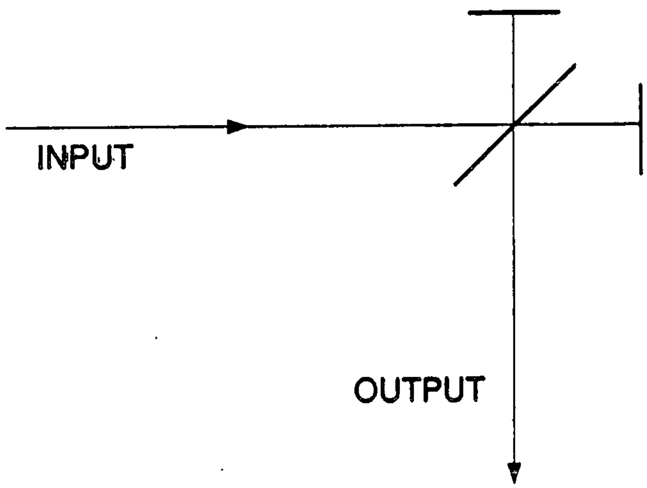

•Output dark for all wavelengths if dark for any.

Introduce asymmetry by shifting one mirror away from beamsplitter by a (large) integral number of half-wavelengths of green light:

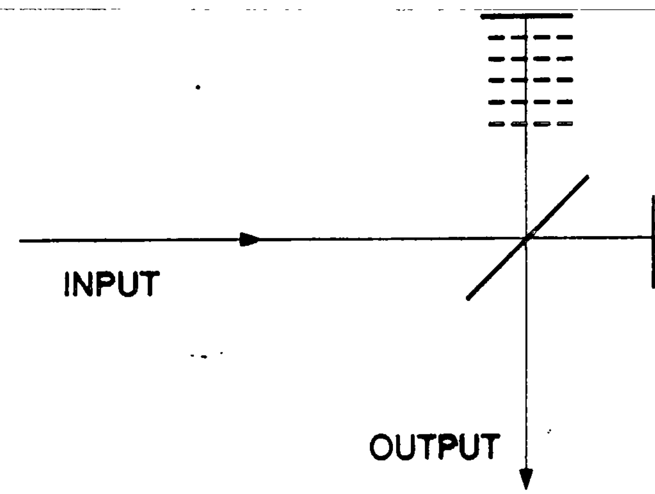

Now output is still dark for carrier, but not for RF sidebands.

•Gravitational wave distorts interferometer, causing carrier to appear also at output: AM produced by beating together of carrier and sidebands.

Asymmetry Scheme

Note: In the language used to describe modulation above, the AM produced is due to the fact that the RF sidebands at the output are shifted in phse by +/- 90° respectively. Carrier is also shifted in phase, by +90°or - 90°, depending on direction of gravitational deformation of interferometer.

Auxiliary Sensing

Need also to detect $L_1 + L_2$ (Average arm cavity length), $l_1 + l_2$('Average recycling cavity length') and $l_1 - l_2$ ('Michelson near mirror difference').

Average Arm Cavity Length

•Carrier phase (but not sideband phase) changes when arm cavity length changes, producing amplitude modulation in recycling cavity

Average Recycling Cavity Length

•Carrier phase changes at a different rate from that for the sidebands when recyling cavity length changes

Michelson Near Mirror Difference

•One RF sideband grows in amplitude, and the other shrinks, when one cavity is moved nearer the beam splitter and the other moved away

Asymmetry Scheme

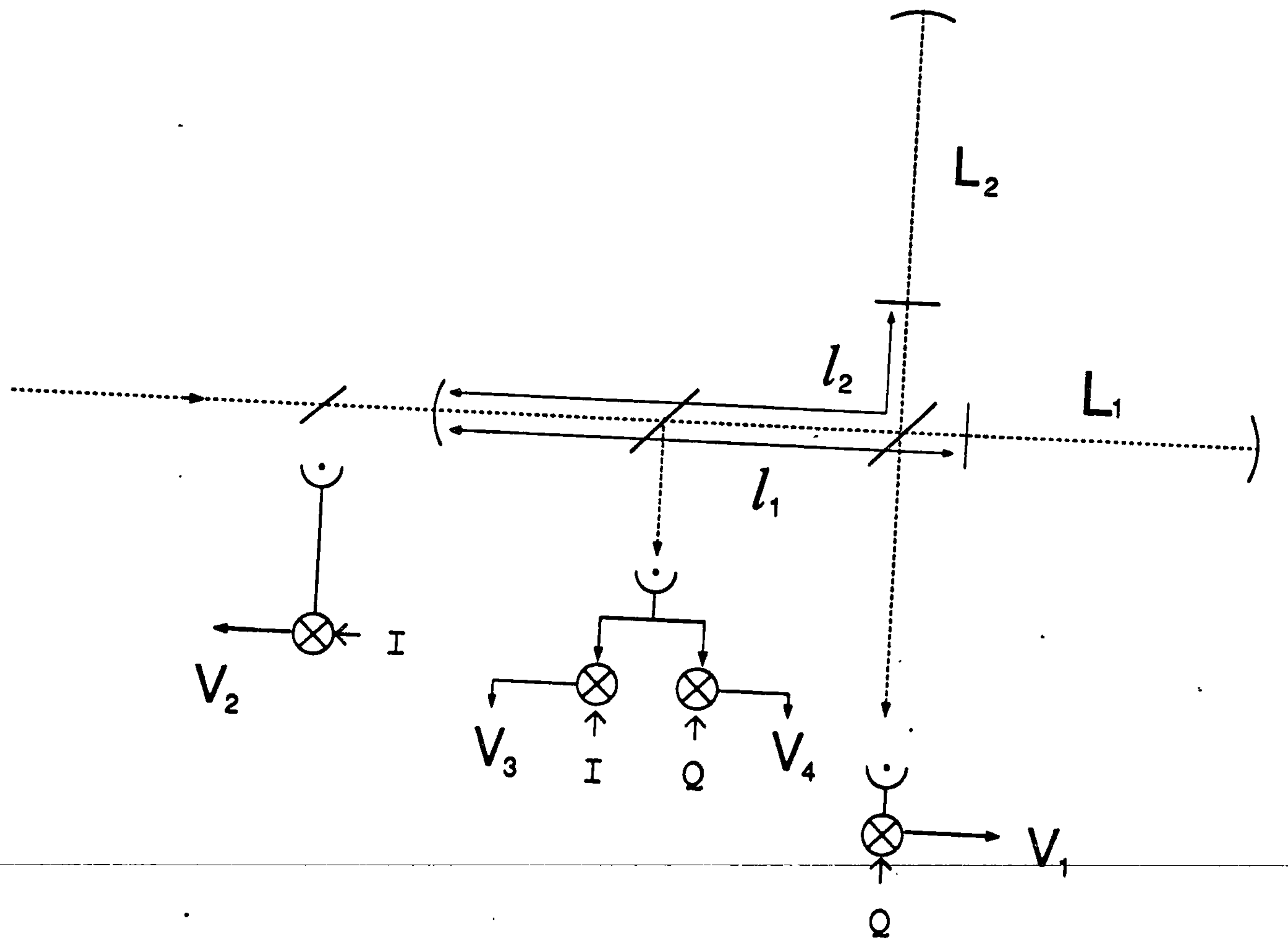

$V_2 \propto \delta L_1 + \delta L_2 + \varepsilon_2(\delta l_1 + \delta l_2)$
$V_3 \propto \delta L_1 + \delta L_2 + \varepsilon_3(\delta l_1 + \delta l_2)$
$V_4 \propto \varepsilon_4(\delta l_1 - \delta l_2)$

Locking Techniques

• Once gains and phases set correctly, prototype acquires automatically when beam splitter is swept back and forth. Mechanism not understood.

• To set gains and phases initially, adjust them in one loop at a time, in the following order:

- laser servo loop (most important)
- differential arm cavity loop
- recycling mirror loop
- Michelson near mirror difference loop

During the procedure, the power circulating in the recycling cavity is monitored by storage scope to measure (and maximize) the length of locked stretches.

III. External Modulation with Subcarrier

- Subcarrier detection of auxiliary interferometer lengths.
- An auxiliary Mach-Zehnder interferometer to detect the gravity wave signal.
- Tabletop experiment at MIT, using LIGO-like cavity finesses.
- Basic scheme for servo control verified; matrix of DC discriminants measured.

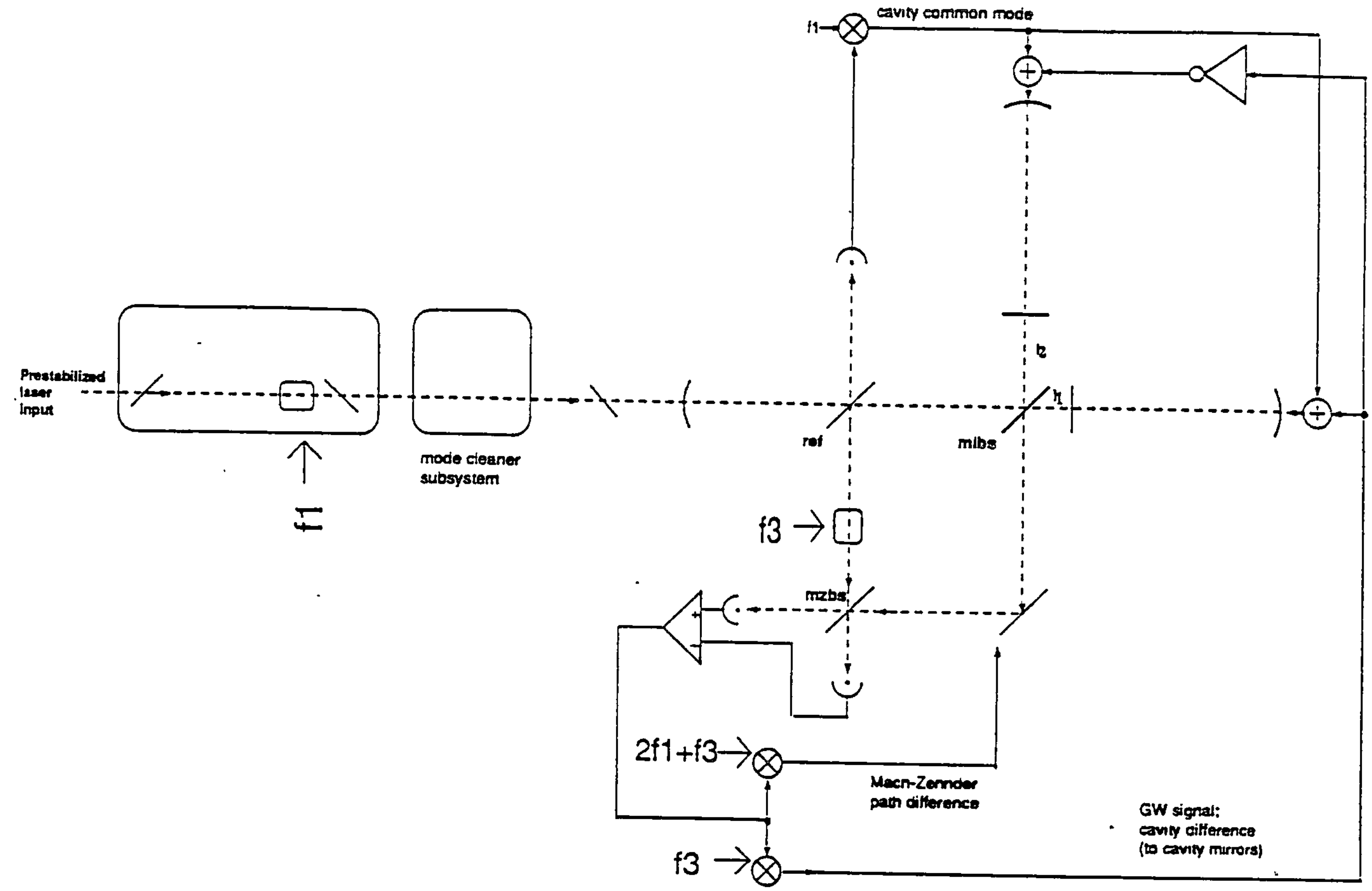

Sum / Difference Cavity Length Readout:

Sum: Reflection discriminant from two cavities.

- Pick off portion of carrier light from symmetric michelson output.
- Photocurrent at f_1 proportional to the sum of arm length errors

Diff: Mach-Zehnder detector.

- Phase of carrier from MI antisymmetric output contains the difference between the length errors of the arms.
- Use auxiliary, Mach-Zehnder, interferometer to measure it.
- Antisymm MI carrier light interfered with a f_3 modulated reference beam from recycling cavity.
- Photocurrent f_3 term proportional to the arm diff signal.

M-Z balance.

- f_1 sidebands of the main beam don't couple into cavities.
- Small Michelson length asymmetry allows some f_1 to leave AS port.
- Most f_1 leaves symmetric port: some is reflected by pickoff, is phase mod'd at f_3.
- M-Z interferometer with these beams: $2f_1 + f_3$ term gives MZ phase error.

J6/2

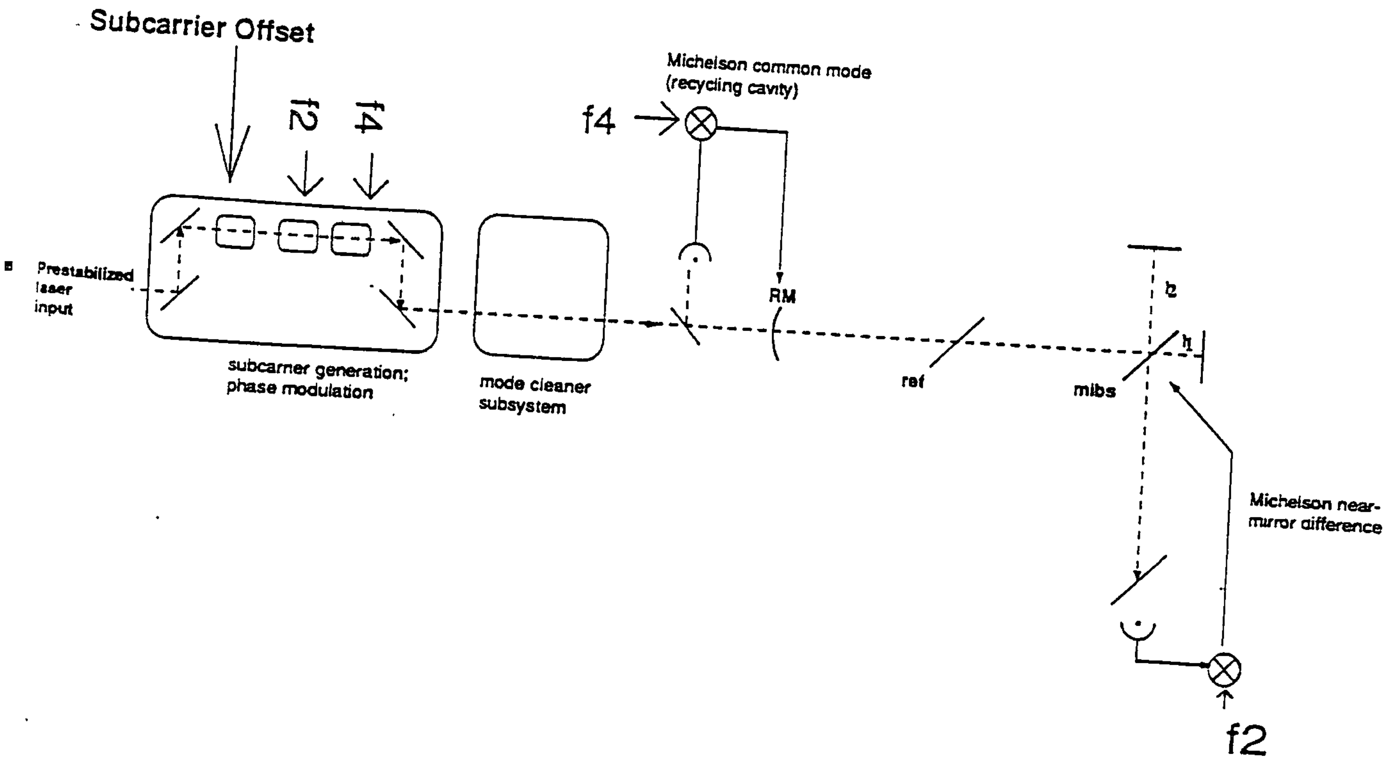

Subcarrier detection of RC & MI lengths:

Subcarrier:

- Inject additional, externally phase modulated, "color" of light, not resonant in the storage arms.
- Offset of subcarrier from carrier's PM frequencies integral number of RC free spectral ranges.
- Subcarrier phase modulation frequency an integral (not half-integral) number of RC FSR's for sidebands to enter the RC.

MI imbalance:

The subcarrier and its f_2 sidebands are used via the Schnupp/ "asymmetry" method to detect the near mirror to BS imbalance.

RC length:

The subcarrier and its f_4 sidebands are used in reflection from the recycling mirror to detect the error in the RC length.

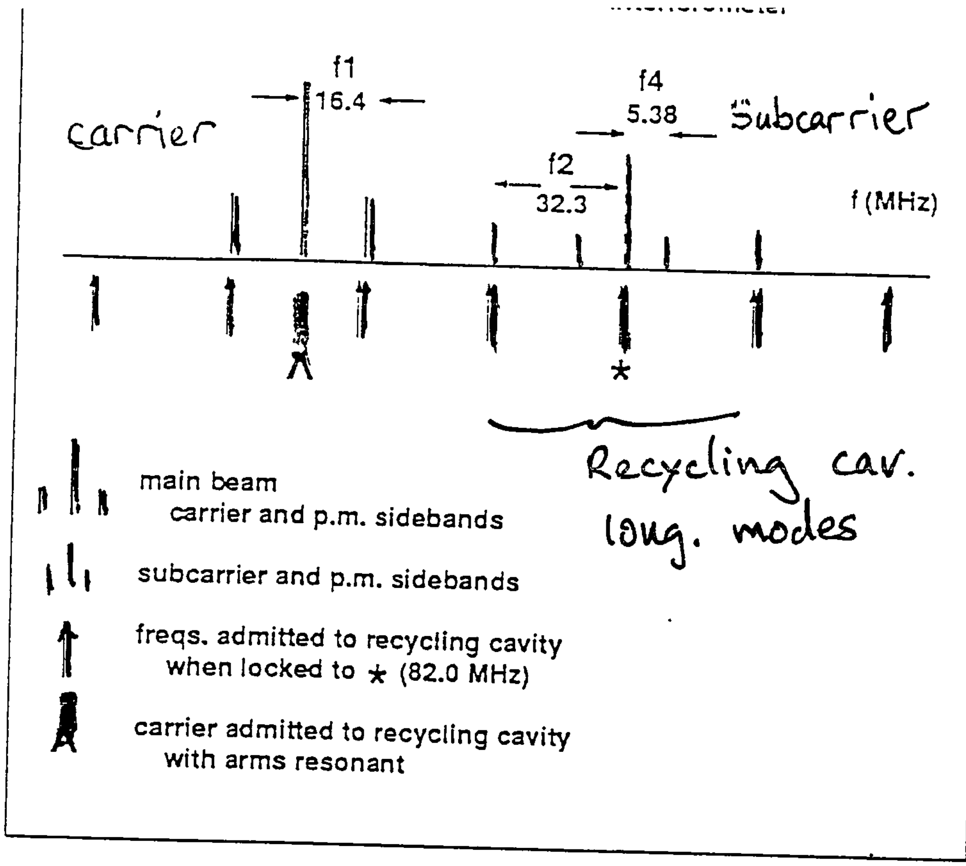

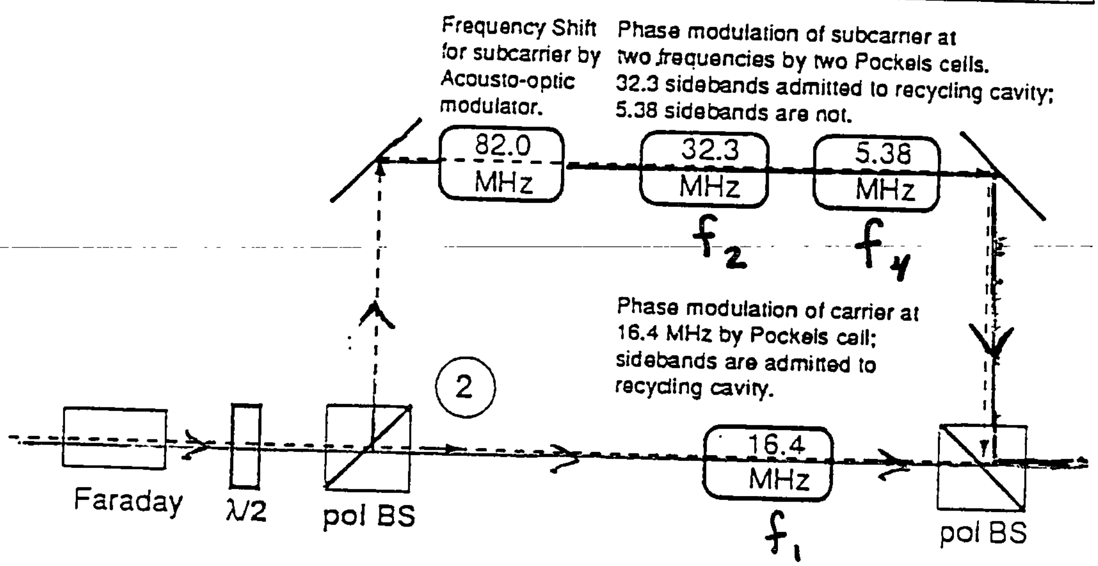

MIT Tabletop Experiment

Arm lengths 30 cm

Recycling cavity length 5 m

Near arm mirror transmission 2.7%

Recycling cavity transmission 14.4%

Modulation Depths: $\Gamma_1 = 1.04$ $\Gamma_2 = .9$ $\Gamma_3 = .9$ $\Gamma_4 = .67$

Light power $\approx 3\,\mathrm{mW}$ each beam.

Key to light frequencies in the hybrid interferometer: Asymmetry GW readout, Subcarrier auxiliary length readout.

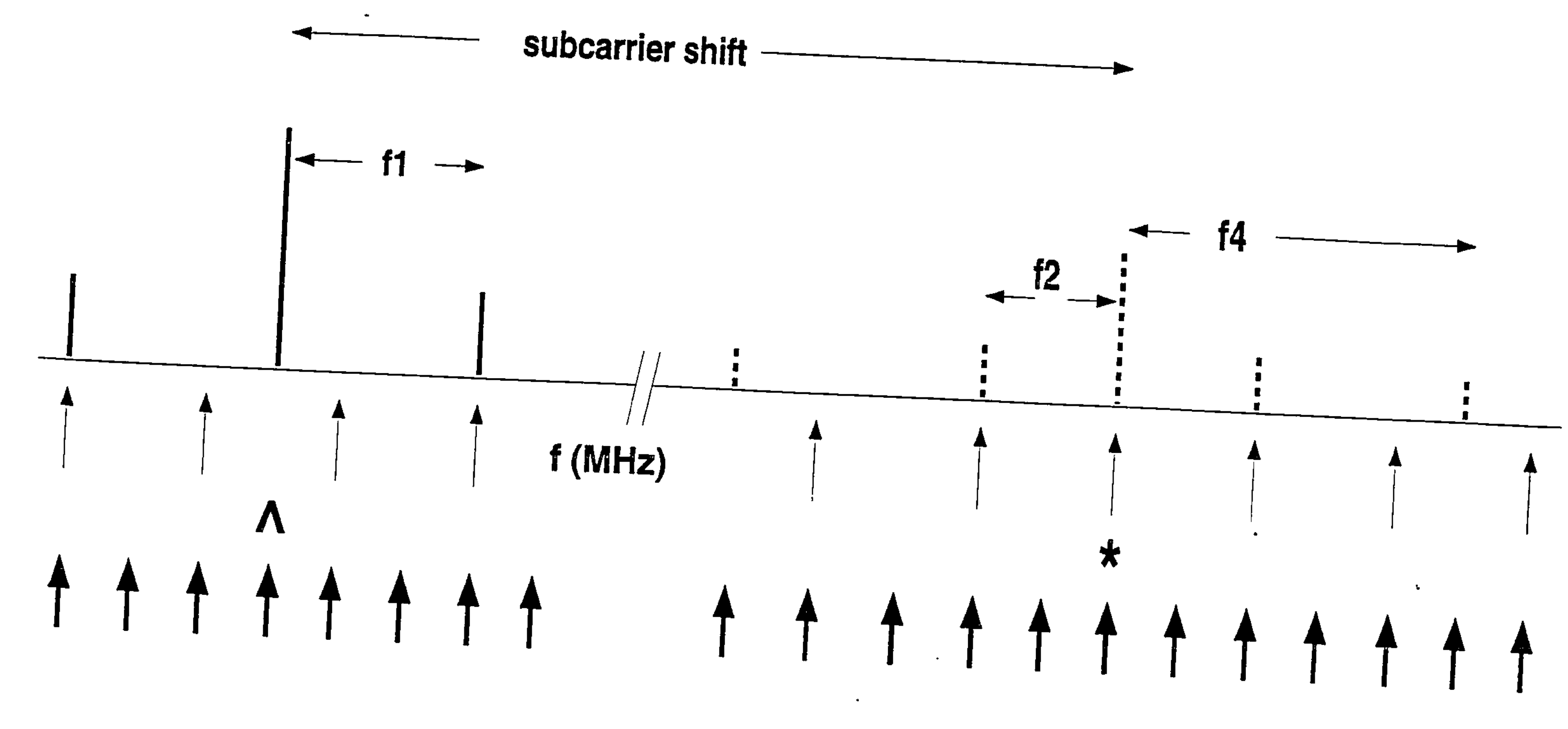

main beam carrier and p.m. sidebands

subcarrier and p.m. sidebands

freqs. admitted to recycling cavity when locked to * .

Λ carrier admitted to recycling cavity with arms resonant

freqs which pass through the mode cleaner, if its length is twice the recycling cavity's.

Possible LIGO Values:

f1 = 3c/2l_rc = 3 * 6.28 MHz

f2 = 2 * 6.28 MHz

f4 = 5 * 6.28 MHz

subcar shift = 250 MHz

J. Giaime 9-23-93

J6/5

Shot Noise

- Gravitational Wave sensitivity: MZ and asymmetry scheme identical to within about 5% for reasonable values of parameters such as loss and contrast defect.
  Note: one possible exception revealed by recent modeling.

- Michelson Near Mirror difference signal: No strong argument here for choice of auxiliary sensing scheme.
  Shot noise level not well established; importance of this noise depends on loop shape and ability to subtract noise out of Gravitational Wave signal.

- shot noise in remaining two degrees of freedom to be sufficiently low to be unimportant

Low- and High-Frequency Response

Asymmetry Scheme

- Low frequency: simple computer model verified in coupled-cavity experiment and by comparison to analytic calculations, and partially tested (one input-output pair) in full interferometer.

- High frequency: no experimental tests. Computer model agrees accurately with low frequency model and qualitatively with analytic calculation.

Mach-Zehnder / FSSC Scheme

—> J. Giaime continues...

J. Giaime September 29, 1993

Measurements of the low-frequency discriminant matrix

What the discriminants are designed to measure

There are five discriminant signals.

- Carrier-derived:
  - Arm cavities, common mode (laser correction)
  - Arm cavities, differential mode (Gravity Wave)
  - Mach-Zehnder fringe centering
- Subcarrier-derived:
  - Recycling cavity, common mode (RC length)
  - Recycling cavity, differential mode (BS position)

The subcarrier-derived discriminants should be (to the extend that the subcarrier is rejected by the arm cavities) independant of the arm lengths, and (to the extent that the main BS $R = T$) orthogonal to one another.

Test signals applied to the system

Small 20 kHz signals were applied to the system in the following combinations:

- Differentially and common mode to rear mirror PZTs
- Differentially and common mode to near mirror PZTs
- to the extra Pockels cell in the Mach Zehnder

The second item describes a drive which should be measured by both carrier and subcarrier discriminants.

calibration of detector systems

The various stages were calibrated as follows.

- The photodiode tuned transformers and preamp boxes were calibrated to photocurrent with shot noise.
- The phase sensitivity of the MZ detection was calibrated with the MZ pockels cell.

J6/1

- The sensitivity of the RC differential loop (without recycling) was calibrated by sweeping the Michelson through a fringe and measuring the discriminant excursion.
- The motion of the near mirror PZTs was calibrated using a simple unrecycled Michelson interferometer and readout calibrated in the last step.
- With the arms blocked and the Michelson held by hand to a dark fringe, the RC was swept to calibrate its discriminant.
- With the entire FMI locked, the calibrated mirrors were used to calibrate the cavity discriminants and the RC discriminants.
- The rear mirrors were assumed to have the same motion/drive as the near ones

J6/2

Measurement of the Discriminant Matrix at 20 kHz.

Test signal to mirrors. With servo loops closed, 20 kHz signal added, in either differential or common mode, to the front or back mirror PZT-mounts, or to the M-Z arm Pockels cell.

Measurement challenges. Optical readout scheme designed to orthogonally measure the phase change within the arms and recycling cavity, not mirror motion. BS is not 50/50 for SC.

Drive		Discriminant photocurrent, Amp/m				
		Carrier: Arms		Subcarrier: RC & MI		M-Z
		Diff	Comm	Diff	Comm	
End Mirrors	Diff	**9.4×10^4**	3.2×10^3	$0.5 - 6$	51	
	Comm	2.6×10^3	4.9×10^4	32	$5 - 89$	
Near Mirrors	Diff	7.8×10^4	7.3×10^2	**6.8**	80	2.3×10^3
	Comm	1.7×10^3	3.2×10^4	34.	20.	2.5×10^3
Mach-Zehnder		23	1.3	2.8×10^{-3}	.14	**13.**

Theoretical predictions, using simple models:

MI Diff discriminant using Subcarrier:

$$\frac{di_{RF}}{dl} = \frac{8\pi}{\lambda} i_0 \, J_1(\Gamma_2) \, J_0(\Gamma_2) \sin(\frac{1}{2} K_2 \Delta l) \approx 25\text{Amp/m}$$

Arm Diff discriminant using Mach-Zehnder:

$$\frac{di_{RF}}{dl} = \frac{16\pi}{\lambda T} \sqrt{i_{\text{ref}} i_0} \, J_1(\Gamma_3) \approx 1.1 \times 10^5 \text{Amp/m}$$

Mach-Zehnder phase error discriminant using $2f_1 + f_3$:

$$\frac{di_{RF}}{dl_{MZ}} = \frac{4\pi}{\lambda} \sqrt{i_{\text{ref}} i_0} \, J_1(\Gamma_1)^2 \, J_1(\Gamma_3) \, \sin(2K_1 \Delta l) \approx 39.\text{Amp/m}$$

where, K_i and Γ_i are the wavenumber and modulation index of RF frequency i, Δl is the macroscopic imbalance in the Michelson arms; i_0 and i_{ref} are the input and reference arm equiv. photocurrents; T is the transmission of the near arm mirror; λ is the optical wavelength.

J. Giaime September 30, 1993

Progress in high frequency response measurements of FMI

Measurement goals

- Frequency responses of each discriminant; expectations:
  - Common-mode arm; pole at combined cavity frequency.
  - Differential-mode arm; pole at arm frequency.
  - Common-mode RC; pole at RC freq.
  - Differential-mode RC; flat.
- Investigation of coupling of cavity rear-mirror motion to subcarrier discriminants. We had expected the Kerr cells to introduce phase between the cavity mirrors, which is different from the PZT tests. Any coupling that was due to mirror rocking would be excluded in this test, which could be done at low frequencies.

Experimental status

- Fused quartz Brewster-cut cells have been made and tested. At low frequencies, the phase response to voltage, measured in a recycled simple michelson, resembles a resonance at 10 kHz, followed by a $1/f^2$ rolloff into a noise floor at $10^{-7} rad$.
- To measure the phase response at high (>80 kHz) frequencies requires use of our recycled arm cavities... unfortunately, enough excess noise is generated at low frequencies exceed the FMI's dynamic range.

How to proceed? Possibilities

- Improved Kerr cell mount design.
- Crystal quartz (or other material) Pockels cell in arms.
- commercial Pockels cell in RC.
- more careful characterization of mirror motion on PZTs.

JG/4

Comparison of Length and Optical Asymmetry Effects

Symbol	Quantity	Initial LIGO	40-Meter Prototype	Expected Optical Asymmetry
w_0	spot radius @ input mirror	2.15 cm	2.15 mm	not applicable
z_0	confocal parameter	2800 m	28 m	
(g_1, g_2)	cavity stability parameters	(1, 0.33)		
δ	length asymmetry	60 cm	30 cm	
$1 - C$	contrast defect	7×10^{-8}	1.2×10^{-4}	$10^{-2} - 10^{-3}$
ϕ_A/ϕ_{FP}	relative frequency noise sensitivity	5×10^{-7}	2.5×10^{-6}	$\approx 10^{-2}$
$P_A/\Delta P$	power fluctuation feedthrough	no additional feedthrough in signal band for balanced system		
$\epsilon_{\Delta z}$	static waist error mode amplitude	1.2×10^{-4}	5×10^{-3}	$\approx 10^{-1}$
$\epsilon_{\alpha,\delta}$	static angular error mode amplitude	2×10^{-5}	10^{-3}	

- **Initial LIGO and 40–Meter Prototype estimates assume that interferometer is centered on dark carrier fringe and do not contain extra optical asymmetries.**
- **Expected Optical Asymmetry estimates are for an interferometer without length asymmetry but with optical asymmetries expected of an initial LIGO interferometer.**

V. Open Issues

Effects of higher spatial modes

- all analysis, experiments above performed in limit of only TEM_{00}
  - misalignments can complicate
  - mirrors, substrates not perfect

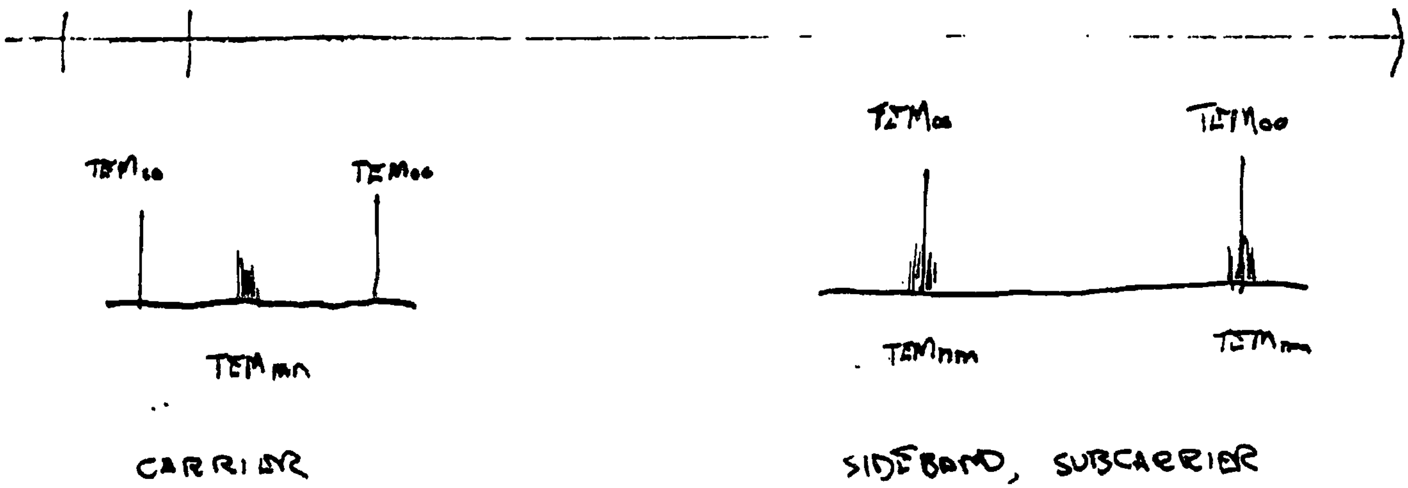

- recycling cavity
  - very good mode cleaner for carrier light
  - almost perfectly degenerate for sidebands, subcarriers
  - AND almost plane parallel—scattering out of TEM_{00} very effective
- Consequence for Asymmetry GW readout:
  - power scattered out of TEM_{00} sidebands
    ($\approx$20% for $\lambda/300$ Zernike on one mirror)
  - excess light on photodetector
  - reduced effective modulation depth
  - possible higher order effects

more Effects of higher spatial modes

- arm cavities
  - imperfect input mirror couples TEM_{00} power into higher modes

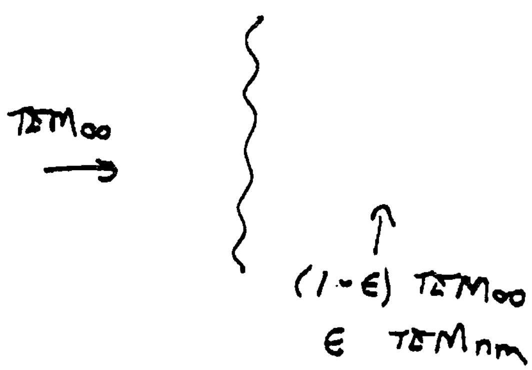

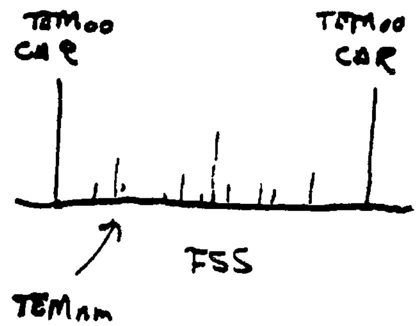

- Consequence for FSS
  - possibility of accidental coupling of FSS to arm cavity
  - field effect, requires only parts in 10^4 coupling to cause trouble
  - either restricts range of cavity lengths, or...
  - could lead to incorrect sign of feedback signal
- Very difficult to obtain relevant experimental results

- Status of modeling
  - numerical model capable of studying effects with real deformations
  - model functions, agrees with simpler models where comparison possible
  - some results for degeneracy of recycling cavity
  - no data yet on FSS arm coupling

- 'corrective optics' may help
  - diaphragms
  - index step in mirror
  - curve on arm input mirror

Other imperfections in the optical system

- some ‘balanced imperfections’ studied
  - contrast defect, in carrier and sideband
  - arm cavity loss
  - splitter ratios
- little study of ‘imbalanced imperfections’
  - arm cavity storage time
  - arm cavity loss
  - beamsplitter ratio
- could impact linear coefficients in sensor →actuator encoding
- SNR considerations
- aid in choice of FSS or Asymmetry aux length readout

- modeling possible, not yet done

Method for generating Frequency Shifted Subcarrier

- in FSS technique, must create beam
  - shifted by up to 300 MHz
  - reasonable efficiency to obtain reasonable SNR for sensing
  - spatially pure TEM_{00} output beam
  - satisfactory frequency, amplitude, pointing noise
  - co-linearity with main beam

- present FMI uses single-passed Acousto-Optic
  - 82 MHz
  - ≈50% efficiency; 80% possible
  - poor output beam shape

- alternatives
  - electro-optics:
    prototype built, 12% eff., ok beam
  - FP locked in transmission on phase-modulator sideband
    prototype built, 35% max. possible eff., very nice output beam
  - second laser, frequency locked to main carrier laser
    allows high FSS power, good SNR
    technically 'heavy' solution, certainly possible

- preferred solution:
  - double passed AO, passed through Mode Cleaner
  - meets criteria above
  - BUT not tested on a prototype (FMI or otherwise)

Acquisition of locked state

- locking of FMIs not well understood
  - Asymmetry FMI requires simultaneous 'lock' of 4 DOF
  - FSS FMI requires simultaneous lock of 2 DOF (arm cavities)

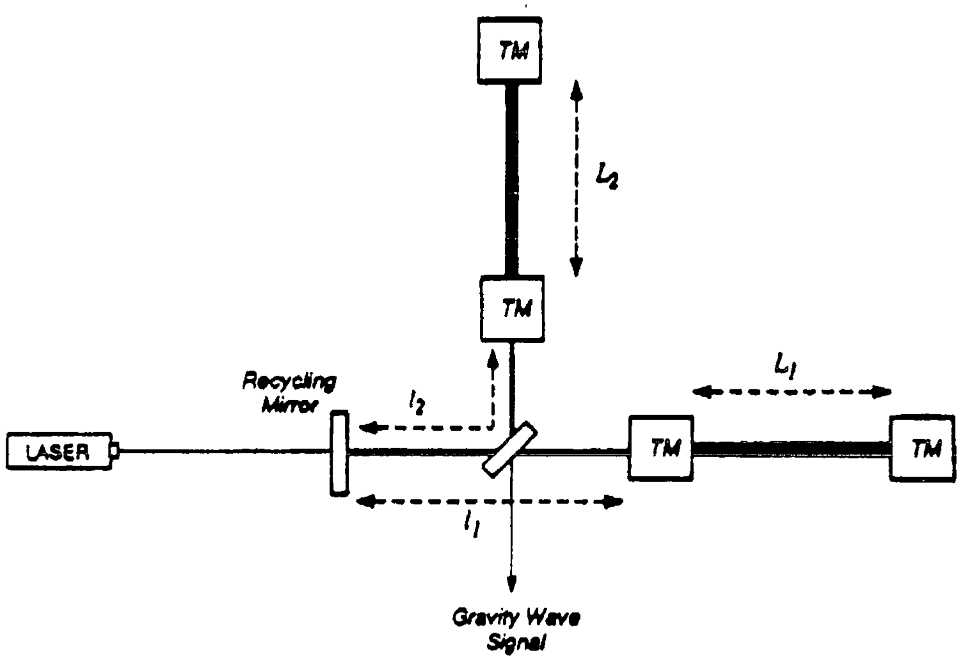

- modeling problem is hard
  - nonlinear (mirrors are moving by tens of individual linewidths)
  - 6 independent mirrors
  - system dynamics strong function of resonance
- reasons to hope
  - both FMIs do lock, so possible (some range of lengths works)
  - experience and modeling of 40m cavities helps
  - countable number of cases
  - phase lock loop theory may help
- needs serious modeling
  - matlab-based time-domain model
- needs tests on suspended interferometer

DHS/5

L. Sievers
9/93

Servo Loop Design for Asymmetry Scheme

- Main issue in servo design is signal strength of recycling cavity signals (same issue experienced in controlling a coupled cavity)
- Want to use V_1 to control ΔL and V_2 to control Δl but both ε_1 and ε_2 are small; ΔL signal dominates both V_1 and V_2.

$\Delta L >> \varepsilon_1 \Delta l$
$\Delta L >> \varepsilon_2 \Delta l$

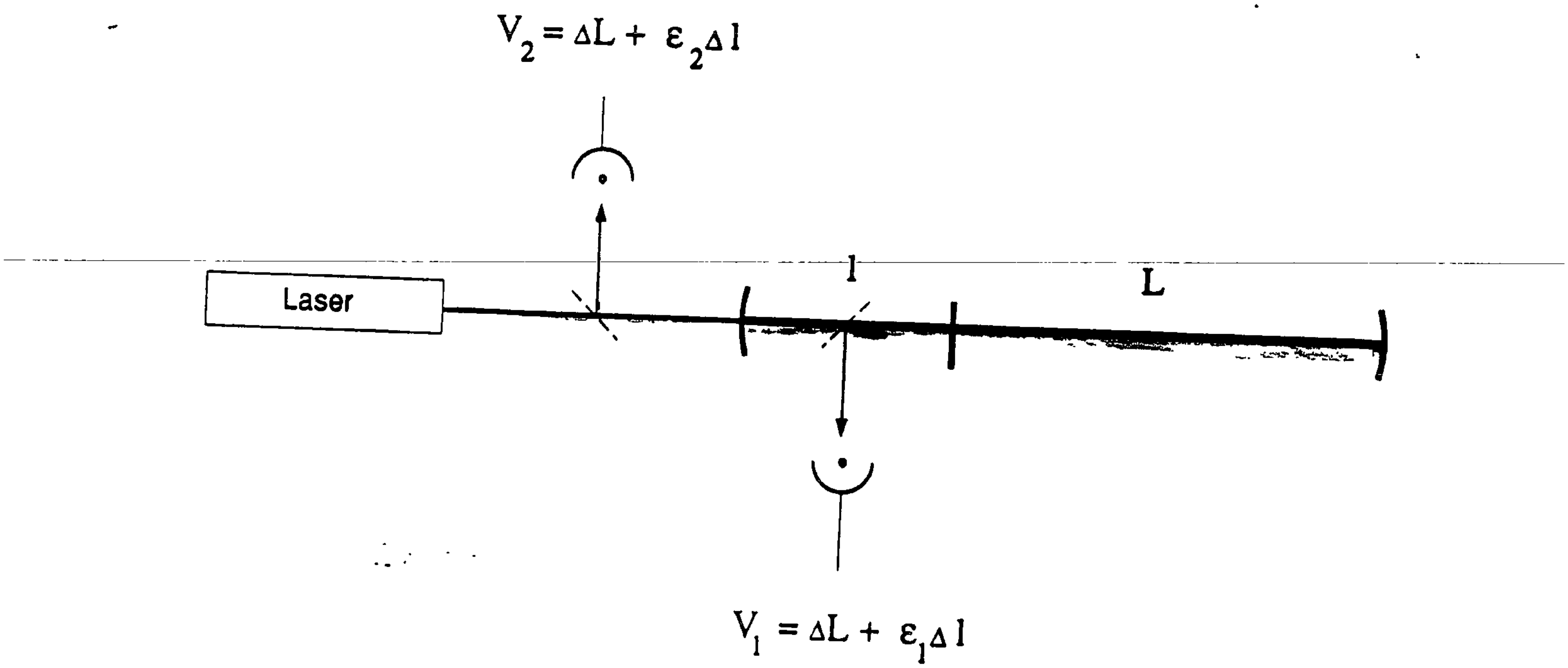

LIGO

Possible Servo Design Scheme:

- Predict that there are no performance compromises if following ratio is satisfied (MR 9/93):

$$\frac{G_1}{G_2} > \frac{1}{\varepsilon_2} \approx 60 - 150$$

- Choose G_2 assuming V_2 sees only signal from Δl
- How to meet above ratio condition ($\frac{G_1}{G_2} > \frac{1}{\varepsilon_2}$):
  - Can't be met if feed V_1 to rear mirror, so will feed V_1 to laser instead
  - Believe high bandwidth of laser loop will allow us to meet ratio condition

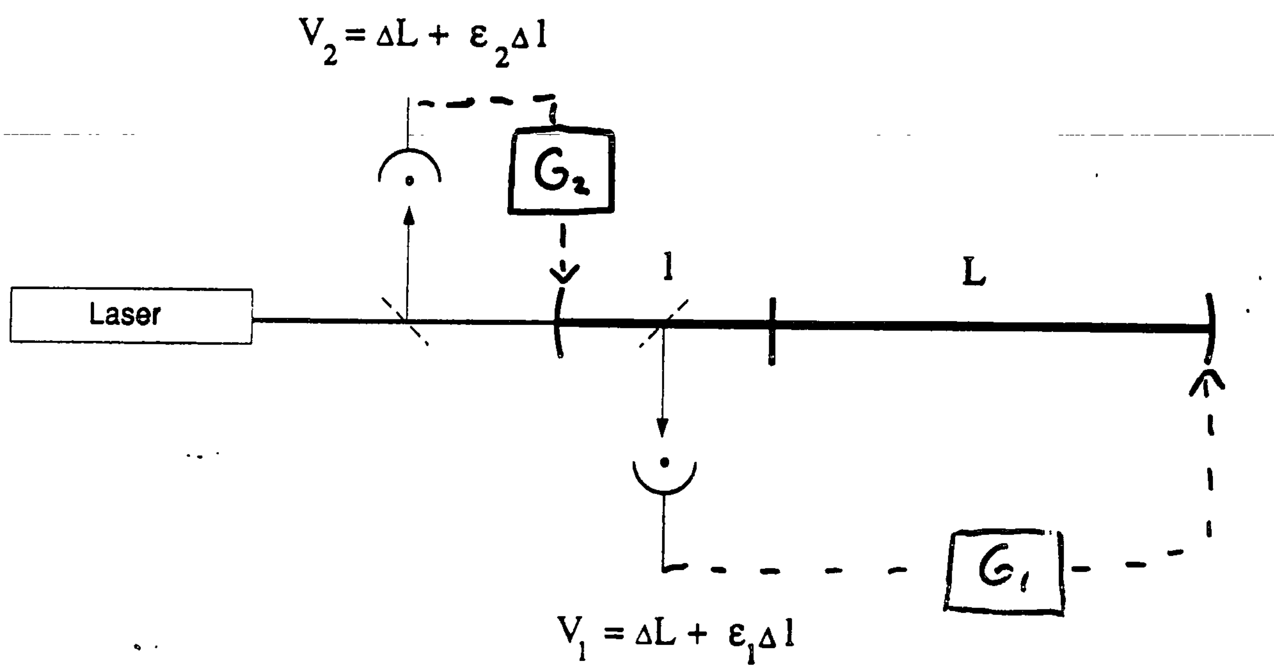

LIGO

Can scale parameters so that feeding back to laser frequency is equivalent to feeding back to end test mass

LS/2

VI. Recommendations

GW Readout: Asymmetry

- Both schemes (asymmetry, Mach-Zehnder):
  - function (show same sensitivity in models and FMI)
  - have similar variation in sensitivity with parameters studied
- MZ does not use sidebands in recycling cavity (possible advantage)
  - has additional components and DOF (disadvantage)

  → recommend simpler scheme: Asymmetry

- caveat: numerical modeling important to carry through
  - test if sideband loss is significant for GW SNR
  - test if variation in sidebands, or of spatial content, problematic

---

Lock acquisition aid: Frequency Shifted Subcarrier (FSS)

- gives independent information for near and far mirrors
- breaks down acquisition sequence, easier to debug
- has moderate technical demand, increase in complexity
- also needs numerical modeling

Operational mode Auxiliary length readout

- Both candidate schemes viable
- FSS: Independence of signals from arm cavities
  - servo design simplified
  - may be troubleshooting aid
- Asymmetry: Simplicity
  - fewer frequencies (carriers and sidebands)
  - simpler hardware (possibly also simpler acquisition FSS)

- **Recommendation: continued pursuit of both approaches**
- neither is exclusive nor requires compromise of other approach
- must develop acquisition FSS in either case
- difference in FSS 'acquisition only' vs. 'operational system' moot
- additional manpower, outlay small for parallel effort
- offers flexibility at runtime

DHS/2

Future R & D — Asymmetry

If Asymmetry not to be used for auxiliary sensing:

- design servo loop for Gravitational Wave degree of freedom

If Asymmetry to be used for auxiliary sensing:

- complete detailed check of high-frequency model against analytic calculation
- measure low-frequency response in remaining degrees of freedom using FMI, and compare to model
- design servo loops for auxiliary degrees of freedom

J. Giaime September 30, 1993

Future directions in FMI research.

Unfinished, necessary, work with present schemes

- Explanation or elimination of rear mirror to FSS coupling.
- Tests of HF response if deemed important.
- Better-controlled complete characterization run.

Tests of chosen scheme

- LIGO modulation frequencies & topology
- FSS generation method
- lock acquisition (better done hanging?)
- investigation of effects of higher order modes?

JG/1

R. Sievers
9/93

Goals of R&D for Optical Modeling of Length Control System

I. Optical model out to a free spectral range for Operational Mode (on resonance)

i. Status

- Completed in-house model (not documented)
- Collaboration with JPL just initiated

ii. Future Work

- Document in-house model
- Work with JPL personnel to complete modeling effort

II. Optical model for lock acquisition

i. Status

- No results to date
- Small effort at both Caltech and MIT
- Collaboration with JPL just initiated

ii. Future Work

- In-house effort should be stepped up significantly
- Work with JPL personnel to complete modeling effort

Goals of R&D for Servo Modeling of Length Control System

I. Servo Model for Operation Mode (on resonance)

i. Status

- Ideas on servo design have been discussed but no analysis has been done

LIGO

MODELING THE FIELD IN A COMPLEX CAVITY.
NUMERICAL SOLUTION
Fast Fourier Transform propagator

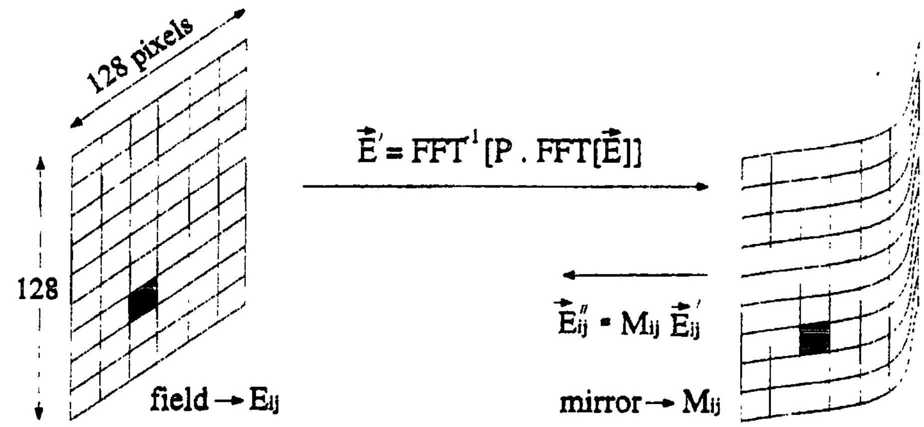

E_{ij} = Electric field of (i,j)th pixel , M = Mirror operator = $r(x,y)e^{j\phi(x,y)}$

FFT = 2-D Fourier transformation , P = free space propagator

THE ALGORITHM

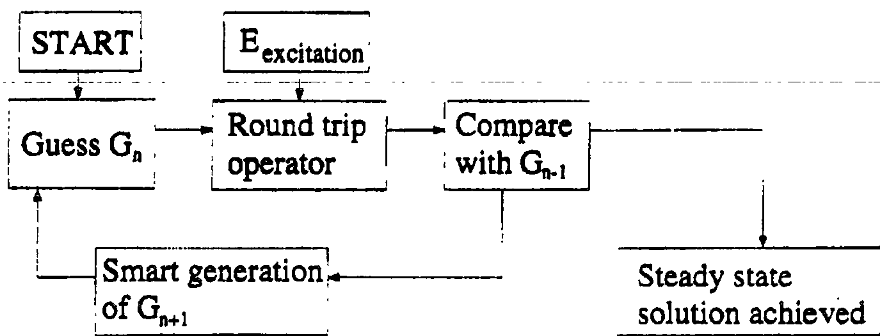

ADVANTAGES:

- **General technique, <u>any type of distortion can be handled</u>.**

DISADVANTAGES:

- **Computation intensive (Cray is needed)**
- **Results give little intuitive understanding. (data points, not relations)**
- **Accuracy is limited by: array size, numerical errors, computation time**

PROGRAM IS READY TO USE WITH FULL LIGO TOPOLOGY

MODELING THE FIELD IN COMPLEX CAVITIES. ANALYTICAL SOLUTION

Hermite Gaussian mode decomposition

1. **THE METHOD:**

   A. **Electric Field:** $E(x,y) = \sum TEM_{m,n}(x,y)\, a_{\,m,n}$

   B. **Optical component operator:** $M_{m,n,k,l} = \int TEM_{m,n} M(x,y) TEM^{\dagger}_{k,l} dx\, dy$

   C. **Free space propagator:** $P_{n,m,n,m} = \exp\left(-k\,\Delta z + (m+n+1)\,\eta(\Delta z)\right)$

2. **SMALL MISALIGNMENT APPROXIMATION**

$$x = \frac{x_0}{W(z)} \ll 1,\ \beta = \frac{\alpha}{\left(\frac{\lambda}{\pi W(z)}\right)} \ll 1$$

<u>**Only TEM_{00}, TEM_{10} and TEM_{01} are needed!**</u>

3. **EXAMPLE:**
   misalignment in the same plane

$$M = \begin{pmatrix} <\psi_{00}|M|\psi_{00}> & <\psi_{00}|M|\psi_{10}> \\ <\psi_{10}|M|\psi_{00}> & <\psi_{10}|M|\psi_{10}> \end{pmatrix} = r\begin{pmatrix} 1-2\beta^2 & 2i\beta \\ 2i\beta & 1-6\beta^2 \end{pmatrix}$$

$$E(x,\beta) = \begin{pmatrix} <\psi_{00} \mid E> \\ <\psi_{10} \mid E> \end{pmatrix} = \begin{pmatrix} 1-\frac{x^2}{2}-\frac{\beta^2}{2} \\ x+i\beta \end{pmatrix}$$

4. **THE FIELD IS GIVEN BY A SOLUTION OF MATRIX EQUATION**
   For two mirror cavity the solution is:
   $E = [I - M_1 P M_2 P]^{-1} t_1 E_0 \quad \mapsto \quad E = M' E_0$
   In a more complex system, one treats a cavity as a single optical element represented by a single matrix M'. The compound system can then be reduced and solved.

   A. **WORK COMPLETED**

   ONE FP CAVITY (agreed with numerical and experientially verified)

   THREE MIRRORS CAVITY (agreed with numerical and experientially verified)

   RECYCLED MICHELSON (agreed with numerical)

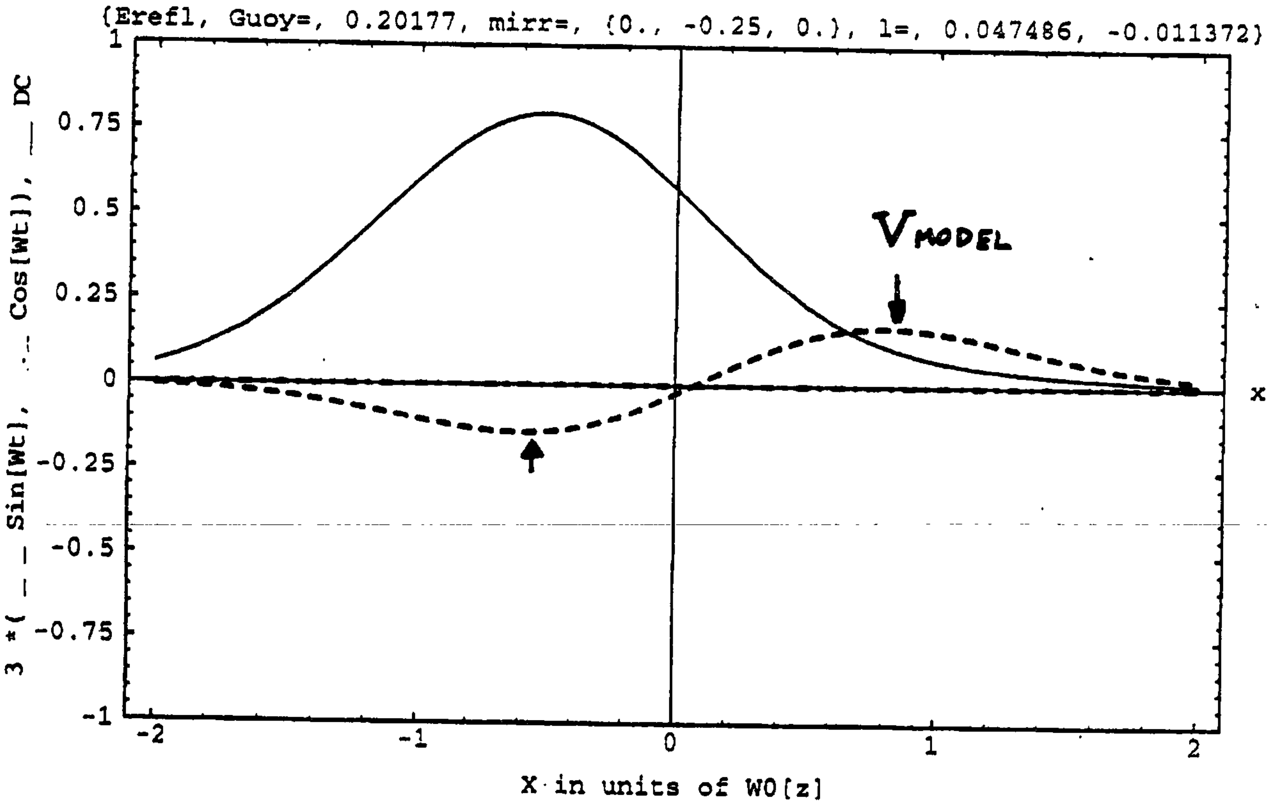
{Erefl, Guoy=, 0.20177, mirr=, {0., -0.25, 0.}, l=, 0.047486, -0.011372}
3 *(_ _ Sin[Wt], _._ Cos[Wt]), ___ DC
X in units of W0[z]
x
VMODEL
1
0.75
0.5
0.25
0
-0.25
-0.5
-0.75
-1
-2
-1
0
1
2

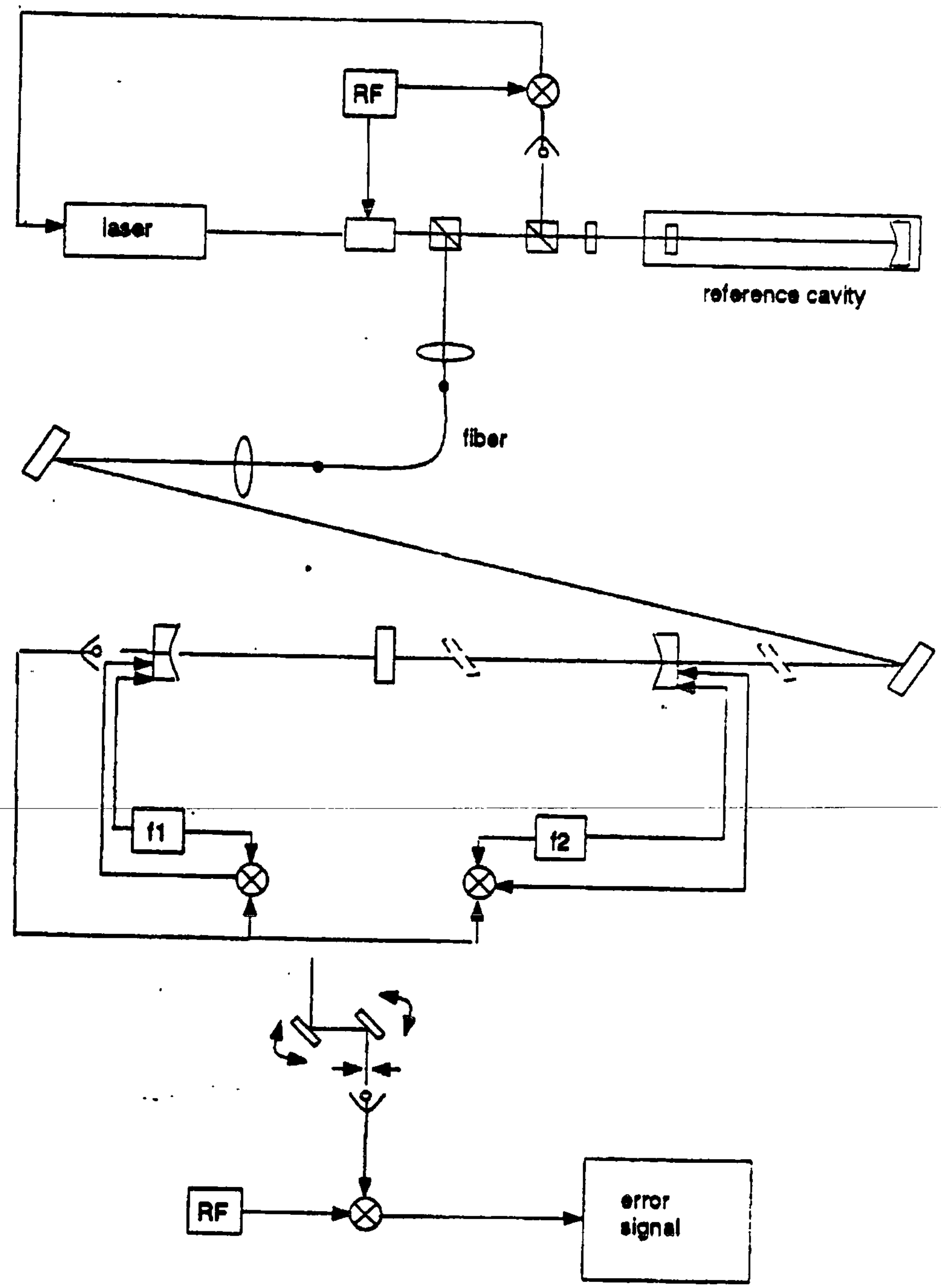

YK/4

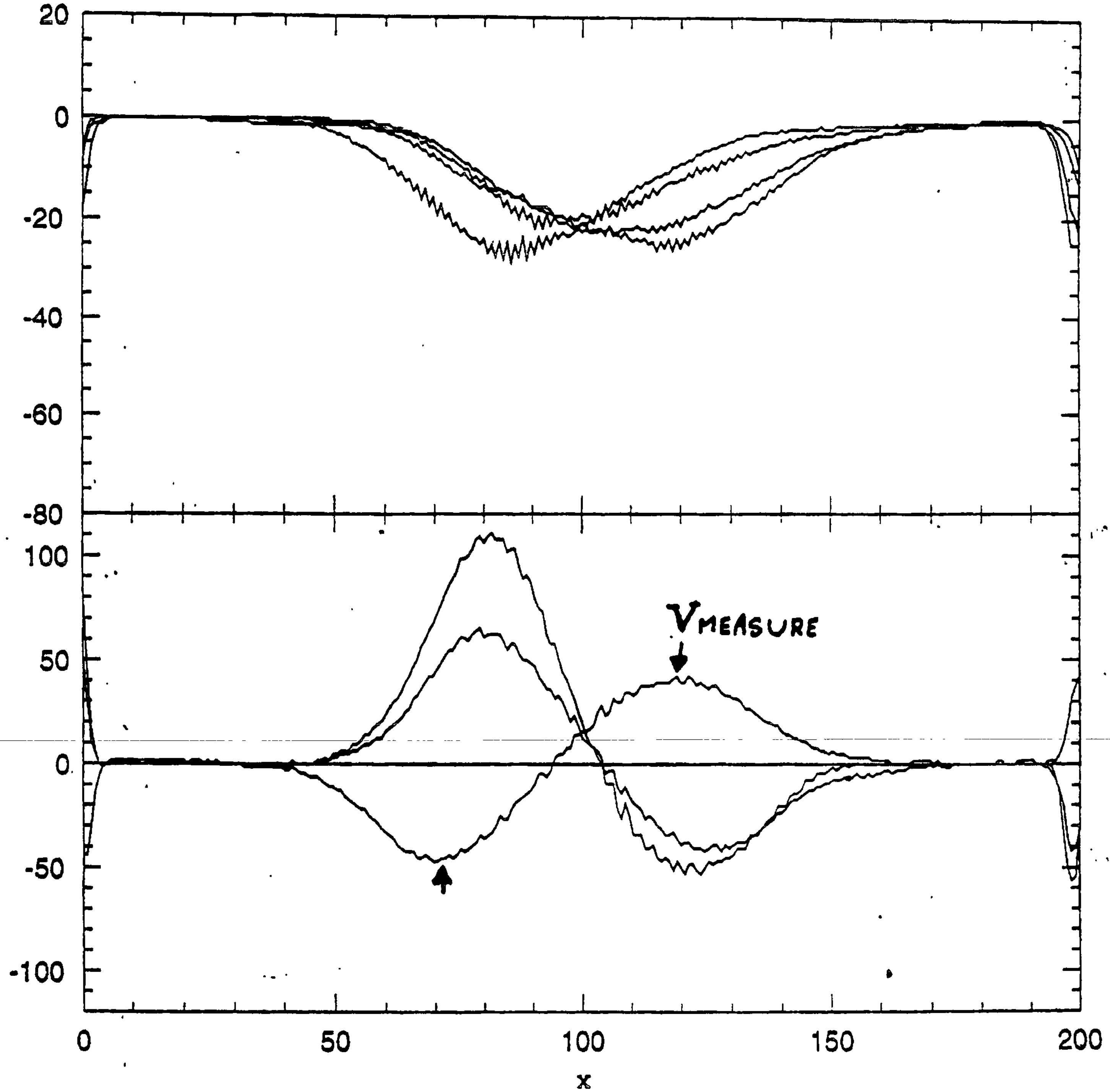

front mirror (d=200 cm)

$\theta_x(\mu\text{radians}) = -155, 0, 310, 465$

YH/5

MIRROR	θ_x (μrad)	NEAR (d = 30 cm)	FAR (d = 200 cm)
FRONT	-155	-45 (0.86)	-85 (1.26)
	310	105 (1.0)	110 (0.82)
	465	130 (0.83)	160 (0.79)
MODEL	23	25	32
MIDDLE	-180	-43 (2.94) ★	-56 (1.64)
	300	35 (1.43)	75 (1.32)
	420	47 (1.38)	105 (1.32)
MODEL	23	6	14
BACK	-197	-40 (1.50)	-73 (1.05)
	296	57 (1.42)	100 (0.96)
	395 (494) →	92 (1.37)	140 (1.01)
MODEL	23	10	26

($V_{MEASURE} / V_{MODEL}$)

YH/6

ii. Future Work

- Once topology has been chosen, need to design servo for prototype and LIGO
- Do analysis of servo design to test for instabilities and noise characteristics

II. Lock Acquisition Model

i. Status

- No analysis

ii. Future Work

- Do analysis to test if servo used for operation mode can be used for acquiring lock
- If not, need to do acquisition servo design

Recommendation for Future R+D Effort in Optical + Servo Modeling

- Presently have a number of somewhat disjoint modeling efforts in progress
- Once LIGO topology has been chosen, need to develop a unified program for optical + servo modeling between MIT, Caltech, + JPL collaborators.

LIGO

Some consequences of asymmetry signal extraction for the ϕ-noise interferometer:

Recycled MI

$T \simeq 1\%$

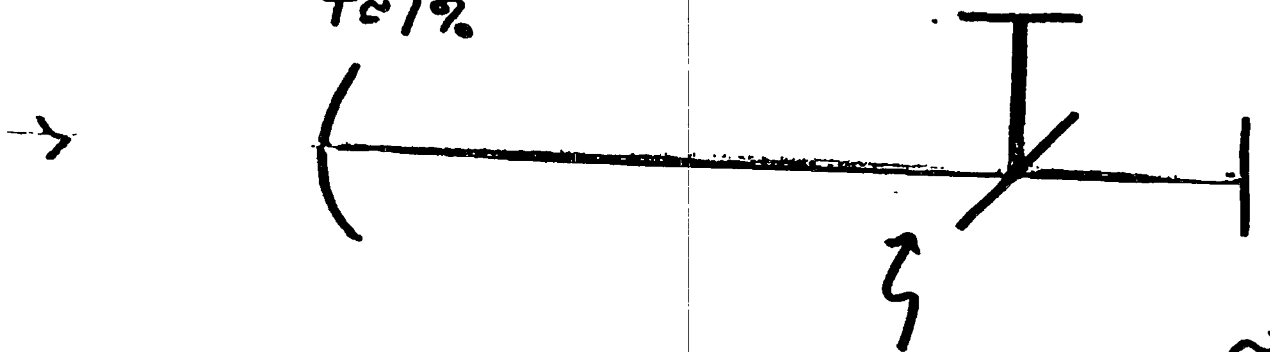

Asymmetry required:

$\sin^2 2k_{rf}\Delta l \sim 10^{-2}$

$f_{rf} \sim 25$ MHz

$\Delta l \sim 10$ cm

$\sim 70\,W \rightarrow \delta\tilde{\phi}_{sn} \simeq 10^{-10}\ \mathrm{rad}/\sqrt{Hz}$

Freq. noise:

$\delta\tilde{\phi}_{\nu} = 4\pi\,\delta\tilde{\nu}(f)\,\frac{\Delta l}{c} < 10^{-10}/\sqrt{Hz}$

requires $\delta\tilde{\nu} \leq 5\times10^{-3}\ \mathrm{Hz}/\sqrt{Hz}$ $\Rightarrow$ need to use recycling cav., eventually mode cleaner for ν-reference

Mode matching loss: $< 10^{-3}$

Beam wiggle....?

PF/1

Topology Tests in 40–Meter Prototype

- Lock Acquisition
  - — characterization
  - — comparison with servo modeling
  - — evaluate necessity of subcarrier for reliable lock acquisition
  - — evaluate utility of subcarrier for diagnostic purposes
- Run Mode Operation
  - — characterization of noise sources and sensitivity
  - — characterization of optical properties, power handling capability
  - — comparison with servo modeling
  - — evaluate necessity of subcarrier for run mode operation